Hindawi
Geofluids
Volume 2021, Article ID 3272860, 15 pages
https://doi.org/10.1155/2021/3272860

Research Article

A Novel Data-Driven Model for Dynamic Prediction and Optimization of Profile Control in Multilayer Reservoirs

Wei Liu,[1] **Hui Zhao**,[1] **Xun Zhong**,[1] **Guanglong Sheng**,[1] **Meilong Fu**,[1] **and Kuiqian Ma**[2]

[1]*School of Petroleum Engineering, Yangtze University, Wuhan 430100, China*
[2]*CNOOC China Limited Tianjin Branch, Tianjin 300000, China*

Correspondence should be addressed to Hui Zhao; zhaohui@yangtzeu.edu.cn

Received 15 May 2021; Revised 12 September 2021; Accepted 7 October 2021; Published 29 November 2021

Academic Editor: Guozhong Hu

Establishing reservoir numerical simulation and profile control optimization methods considering the mechanism of profile control has always been a difficult research problem at home and abroad. In this paper, firstly, a physics-based data-driven model was established on daily production data of injection and production wells following the principle of material balance. Key parameters including transmissibility, control pore volume, water injection allocation factors, and injection efficiency are derived directly from history matched model, and the dominated flow channels could be quantitatively identified. Then, combined with the evaluation results of the plugging ability of the plugging agent, imaginary well nodes are added to the existing interwell relationship to characterize the heterogeneity of interwell-specific parameters. This process performs flow processing along the interwell control units, forming a new and rapid method for simulation and prediction. Lastly, based on the calculated interwell transmissibility, water injection efficiency, and allocation factors, injection wells with low water injection efficiency can be preferentially selected as profile control wells. In addition, taking the production rates, injection rates, and the amount of plugging agent as optimization variables, we established an optimal control mathematical model and realized the parameter optimization method of the profile control. We demonstrated the results of one conceptual model and two indoor experiments to verify the feasibility of the proposed method and completed two actual field applications. Model validation and actual field application show that the proposed method successfully eliminates the complicated geological modeling procedure and the tedious calculation process associated with the profile control treatment in traditional numerical simulation methods. The calculation speed improves tens or hundreds of times, and water channeling paths are accurately identified. Most importantly, this method realizes the overall decision-making of profile control well selection, dynamic production prediction, and parameter optimization of profile control measures quickly and accurately by mainly using the daily production data of wells. The findings of this study can help for better understanding of the optimization design and application of on-site profile control schemes in large-scale oilfields.

1. Introduction

At present, water drive is still the main development method for most oil fields in the world. However, the injection-production contradiction is nonnegligible. On the one hand, the low permeability nature of the reservoir always leads to a high water injection pressure and desperate lack of formation energy replenishment. On the other hand, the existence of multilevel preferential seepage channels in the reservoirs provides more chances for serious water logging and channeling.

The increasingly prominent injection-production contradiction makes the multilevel predominant flow field in low-permeability reservoirs difficult to identify [1–3]. To relieve the contradiction and reduce the adverse effects of water logging/channeling, profile control gradually becomes an indispensable supporting technology for water flooding. Though there are many experimental studies on profile control treatment including formula construction and process design, the numerical simulation related to this area is still in infancy. Thanks to the difficulties in precise modeling

and prediction of dynamic profile control parameters, inadequate acknowledgement of reservoir connectivity, and inaccurate identification of preferential seepage channels, the on-site profile control operation usually shows unsatisfying results and short valid period. Considering the low oil price and to reduce the operation cost, it is important and urgent to conduct effective profile control operation at the right time with optimized parameters.

The key to optimize the profile control operation in low-permeability reservoirs is first to accurately simulate and predict the dynamic reservoir performance considering the profile control operation and then to optimize the timing and the operation parameters. Commonly applied methods for profile control prediction are field test, statistical modeling, and numerical simulation [4–6]. Field test method and statistical modeling mainly rely on experiential decision-making without considering the reservoir connectivity; therefore, most operations show poor effects and short valid period [7–10]. Profile control numerical simulation is a subcategory of chemical flooding numerical simulation, and there is much experience that can be used for reference. Chemical flooding numerical simulation has long been a difficulty in the field of reservoir numerical simulation, which possesses the characteristics of multiple components, complicated characteristic parameters, complex functional mechanism, indefinite equation constancy, obvious nonlinear feature, and great difficulty in finding solutions for fully implicit equation sets. Although various chemical flooding theories have been practiced for a long time, the milestone for widely accepted chemical flooding numerical simulation had not been set until the late 1970s when in 1978 G. Pope established a multiphase-multicomponent 1D simulator. The simulator includes the changes of phase state and interfacial tension with the concentration of electrolyte and surfactant, the change of polymer viscosity with the concentration of electrolyte and polymer, and the mechanisms of adsorption, diffusion, and ion exchange during the flowing process. After that, various models for polymer flooding, surfactant flooding, alkaline flooding, and combined flooding are gradually established. In the 1980s, numerical simulation of profile control operation was motivated. The simulation ability has experienced an innovative change from the earliest isothermal simulation on 1D simulator with simple mechanism and single medium to the later nonisothermal simulation on a 3D simulator with complicated functional mechanism (gravity, capillary force, startup pressure, and deformation) and dual medium. The simulated object extends from traditional simple polymer and preformed particle gel to novel systems including delayed crosslinking gel, microgel, inverse emulsion, and microbial flooding system. The solving method varies from normal implicit pressure explicit saturation (IMPES) method to high-order IMPES method, streamline curvature numerical method, dimensions reduction method, etc. Nonetheless, the rapidly updating simulation method remains to be imperfect. The existing shortcomings may include (1) complicated percolation mechanism of profile control agent raises the difficulty in fine reservoir description. (2) Large calculated amount greatly lowers the calculation speed. (3) Insufficient inclusion of information on interwell preferential seepage path complicates the simulation and optimization process. Therefore, the large-scale application has been limited [7–10].

To simplify the calculation process and improve the calculation speed, some scholars use methods such as deep learning to predict the production performance [11–13]. Zhao et al. [14] developed a new physical data-driven model called INSIM. Well location and daily production data are the main required information to build a model using INSIM. In addition, different from machine learning models and other traditional models, rapid dynamic predictions can be made following the principle of material balance and parameters like interwell transmissibility and control volume can be easily derived by history matching to quantitatively show the interwell correlation. Hereafter, some expansive models such as INSIM-FT [15], INSIM-FT-3D [16], INSIM-FPT [17], and polymer channeling prediction model have been put forward [18]. However, the biggest difference between displacing agents and profile control agents is that normal displacing agents like polymer and surfactant generally flow in continuous phase, while profile control agents usually transport in discrete phase and would worsen the heterogeneity between injection and production wells [19]. In the current INSIM method [20, 21], the interwell transmissibility parameters are assumed to be homogeneously distributed, which fails to consider the heterogeneity nature of different interwell correlations. Thus, the exact mechanism of profile modification remains unclear.

Timing and operation parameter are of crucial importance for a successful profile control operation. Therefore, it is meaningful to conduct researches on operation timing selection and parameter optimization. The commonly used decision-making methods are laboratory test method, reservoir engineering method (PI decision-making), and statistical method (fuzzy comprehensive evaluation, BP neural network, support vector machine, etc.). For laboratory test method, a large number of experiments are required to compare the effects of different operation parameters. It may be more accurate at lab scale, but the great difference between core plug or sand pack and real reservoirs makes it unapplicable for direct filed application [22–24]. PI decision is commonly made according to the wellhead pressure index of injection well and some test data. Though simple and applicable, limited decision-making factors being included in the process greatly restrict its practicability. Fuzzy comprehensive evaluation method is developed on the basis of static geological research and water injection dynamics. The values of various decision-making factors are determined, and multiple factors are considered to make a comprehensive decision. However, the weight as well as the subject degree is ambiguous and the effects of subjective factors may be exaggerated. BP neural network method transforms the inputs and outputs into a nonlinear optimization problem, and the weights are obtained by gradient algorithm with iterative operation [25, 26]. This method successfully avoids the difficult problems of weight and subject degree determination encountered by fuzzy comprehensive evaluation method, and the process is automatically continued to get the local optimal solution. Local optimal solution is not representative and may be inaccurate; therefore, the support vector machine

(SVM) method is proposed [27, 28]. The SVM method is designed for finite samples, and oil increment in an operation cycle is the evaluation indicator. The profile control effect-influential factor relational model is built to predict the optimal injection amount and the oil increment in an operation cycle. The optimal solution shown in SVM method is the global optimal.

In recent years, great breakthroughs have been made in optimization theory and numerical reservoir simulation-based reservoir exploitation and production optimization technology [29–31]. The objective of this technology is to find the optimal values for operation parameters (injection rate, production rate, and flowing pressure) to guide the manipulation of the production system and therefore to maximize the economic benefits. Its preliminary application has been realized in water-flooding reservoirs for injection-production parameter optimization, but there are scarce reports on dynamic optimization of profile control operation. The core of reservoir exploitation and production optimization technology is algorithm optimization. Gradient algorithm and derivative-free algorithm are two generally applied algorithm types. Adjoint method [32, 33] is the most popular gradient algorithm, by which the gradient of the objective function can be accurately obtained, while the shortcoming is that the necessity of adjoint matrix would greatly complicate the solving process. Derivative-free algorithms, especially Simultaneous Perturbation Stochastic Approximation (SPSA) algorithm [34, 35] and EnOpt algorithm [36, 37], have attracted widespread attention. In SPSA algorithm, all control variables are under simultaneous perturbation and the perturbation gradient is generated. The only calculation involved is the computing process of the performance index function; thus, the reliability of the gradient and the optimal values are ensured. EnOpt algorithm generates a number of normally distributed control vectors based on the current optimum control. Then, these control vectors together with their corresponding objective function values are analyzed to find a correlation and the search direction. Subsequently, control variables are optimized step by step by iterative method. Other derivative-free algorithms such as SID-PSM algorithm [38], NEWUOA algorithm [39, 40], genetic algorithm (GA) [41], particle swarm optimization (PSO) [42], and simulated annealing algorithm (SA) [43] also get some attention, but the calculation efficiency still has a lot of room for improvement. To mitigate this problem, Zhao et al. later on proposed an updated algorithm named quadratic interpolation model-based approximate gradient algorithm (QIM-AG) [44]. Both the converging rate and the stability show notable improvements, and the improved algorithms are conformable for field applications of injection-production parameter adjustment.

In this paper, we involve the functional mechanism and the sweep volume of the profile control agent and put forward an updated INSIM model to study the heterogeneously distributed injection-production interwell-specific parameters. Imaginary wells are added in between two wells to precisely demonstrate the flow characteristics of connected units, and a new method to predict the profile control dynamics of multilayered reservoirs is established. Meanwhile, after parametric inversion, the data-driven model can cooperate with the interwell transmissibility and water injection efficiency and divide coefficient data to screen the low-efficiency/inefficient wells. The optimal solution is given considering the production/optimization method, so the optimal production scheme and profile control design generated can be applied to guide the future development of low-permeability reservoirs. The calculation speed improves hundreds of times, and water channeling paths are accurately identified. Most importantly, well production data are the only requirements for the overall decision-making of the profile control measure, including accurate well selection, rapid prediction, and dynamic optimization, which may shed light on the field-scale project design and the dynamic optimization of key parameters.

The novelty of our work in this paper is that we established a new processing method based on the previous INSIM model combined with the results of laboratory experiments to perform production simulation if plugging control implemented in waterflooding reservoirs and achieved the optimization of injection volume of plugging agent. Compared with traditional numerical simulation methods, the main advantages of the proposed method are as follows: (1) the process of establishing the simulation model is very simple; (2) the calculation speed is very fast; (3) the traditional numerical simulation method based on the grid system needs to consider very complicated seepage mechanism of plugging agent and requires grid refinement, which results in high computational cost and often does not converge. The method we proposed is relatively convenient to deal with profile control of different plugging agents. Our process is to correct the transmissibility, but this change is done instantaneously. Unlike in the grid-based system model, the permeability of the grid around the injection well gradually changes as the amount of plugging agent injected increases.

The research work of this paper mainly includes several aspects. First, the data-driven model is presented to perform history matching, infer the interwell-specific parameters, and calculate injection allocation factors and inefficiency. Then, according to the evaluation results of the plugging performance of the plugging agent in the laboratory experiment, the transmissibility is corrected along the interwell control unit to predict production performance after profile control. Finally, we also established an optimal mathematical model and solved it with suitable optimization algorithm to obtain optimal design of the water injection rate, liquid production rate, and plugging agent injection volume of wells.

2. INSIM Data-Driven Model of Multilayer Heterogeneous Reservoir

2.1. Characterization and Calculation Method of Specific Parameters for Interwell Control Unit. The basic principle of the INSIM method is using a series of connected units characterized by interwell transmissibility (T_{ij}) and control pore volume (V_{pij}) to represent the injection-production system. Interwell transmissibility reflects the average interwell seepage capacity and dominant flowing direction, while

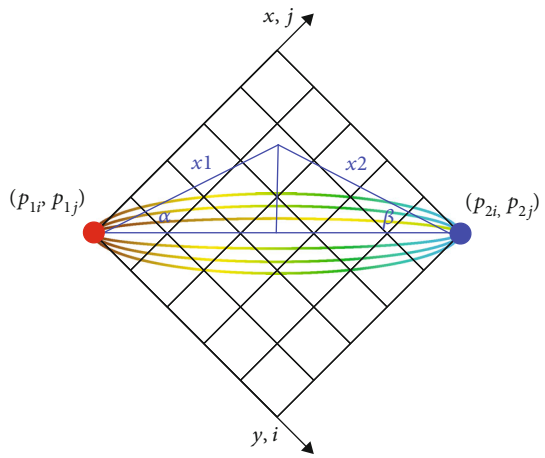

Figure 1: Characterization method of interwell connectivity parameters in heterogeneous reservoirs based on flow tube method.

connected volume represents the material basis of each unit, indicating the interwell water displaced volume. To more accurately calculate the interwell transmissibility and control pore volume for heterogeneous reservoirs, some changes are made on the calculation methods originally proposed by Zhao et al. [14, 17] for homogeneous reservoirs. We assumed that in heterogeneous reservoirs, fluids are flowing in the "flow tube" constrained by different streamlines, as shown in Figure 1. For each "flow tube," the interwell material balance equation is obtained by partial integration of each grid in the cross and longitudinal directions. By applying an interwell equivalent connectivity model, the expressions for interwell transmissibility and control pore volume are given in Equations (1) and (2). The characterization and calculation method of specific parameters for interwell control unit is demonstrated in detail in Appendix A.

$$T_{i,j,k} = \int_0^{\alpha_m} \frac{h}{2\mu\left(\int_{X1}(d\xi/K(\xi)\xi_1) + (\alpha_m/\beta_m)\int_{X2}(d\xi/K(\xi)\xi_2)\right)} d\alpha, \tag{1}$$

$$V_{p,i,k} = h\int_0^{\alpha_m}\left(\int_{X1}\phi(\xi)\xi_1 d\xi + \frac{\beta_m}{\alpha_m}\int_{X2}\phi(\xi)\xi_2 d\xi\right)d\alpha. \tag{2}$$

2.2. Characterization Method of Adding Imaginary Wells in Strong Heterogeneous Reservoir after Profile Control. In this part, the typical one injection-four production well group is taken as the example (Figure 2). First, rational models showing the correlations between plugging agent injection volume, connectivity/permeability/porosity distribution, and plugging agent swept volume are constructed [22]. Herein, the distribution of plugging agent in each connected unit is calculated by divide coefficient and other related parameters, while the swept volume of plugging agent as well as its impacts on reservoir percolation ability is known from the laboratory profile control experiments. The dimensionless plugging agent injection volume of each connected unit is determined by the ratio between the total injection volume

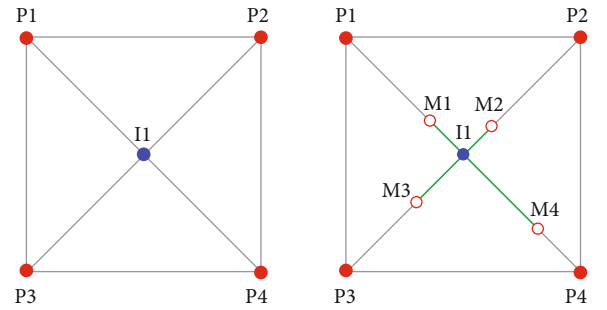

Figure 2: Add imaginary wells to represent the heterogeneously distributed interwell connectivity parameters after profile control operation.

and the connected volume of the target unit. Second, well pattern infilling by imaginary wells is conducted to include the influences of plugging agent. Well locations are determined based on the swept volume, transmissibility, and control pore volume after profile control operation is updated according to the plugging agent injection volume-permeability/porosity distribution rational model and Equations (1) and (2).

2.3. INSIM Data-Driven Model for Multilayer Profile Control Operation. Herein, we give a general sketch of injecting gel or plugging agent to implement profile control, as shown in Figure 3. The purpose of profile control is to block the dominant flow channels to improve the utilization of water injection.

The connectivity feature of multilayer reservoir is integrated into the primary INSIM model [14, 17] to generate an improved data-driven model (Figure 4) for the prediction of multilayer profile control. The production dynamics are calculated by material balance equation based on connected unit, and the connectivity parameters are derived by history match. If the influence of interlayer crossflow cannot be ignored, we can apply the Delaunay triangulation to generate connection map as in 3D dimension by adding a vertical transmissibility between up- and downperforated layer. The initial value of vertical transmissibility could be given approximately according to the actual condition [20].

For well i, the material balance equation is given in Equation (3) [21]. The effects of capillary force and gravity are ignored.

$$\sum_{k=1}^{N_l}\sum_{j=1}^{N_w} T_{i,j,k}\left(p_j(t) - p_i(t)\right) + q_i(t) = \frac{dp_i(t)}{dt}\sum_{k=1}^{N_l} C_{t,k}V_{p,i,k}(t). \tag{3}$$

Equation (3) is discretized using implicit difference method. It is worth noting that the INSIM model does consider the changes and effects of mobility of the flowing fluid. We think that the relationship between $T_{i,j,k}$ and $T^0_{i,j,k}$ depends on total mobility [11, 14, 20, 21]. Assume that the

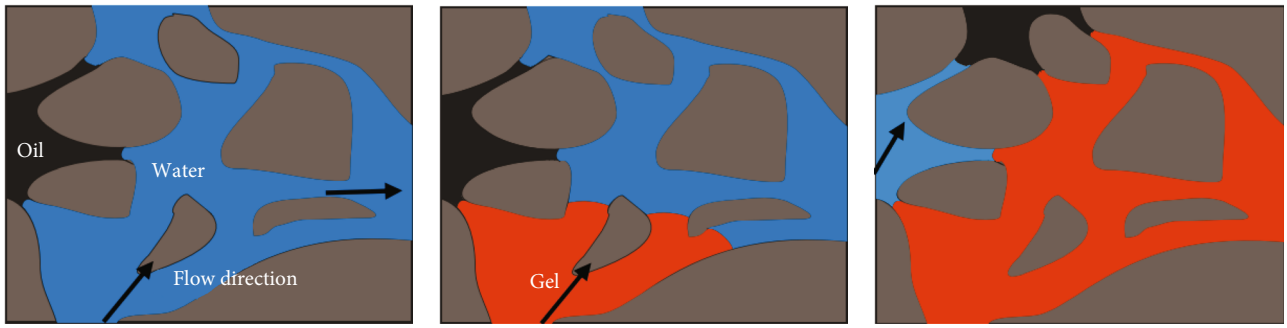

(a) Waterflooding (b) Injection of gel (c) Profile control

Figure 3: General sketch of the problem under study.

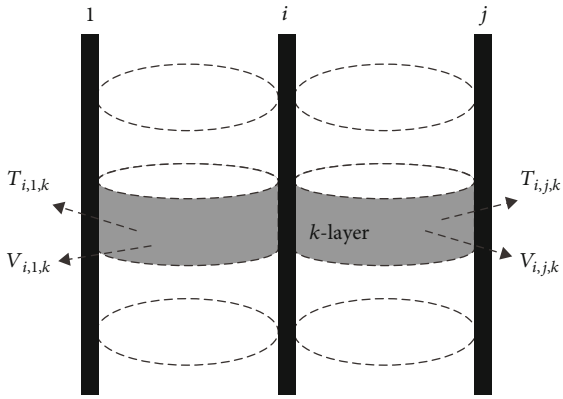

Figure 4: Schematic diagram of connected unit.

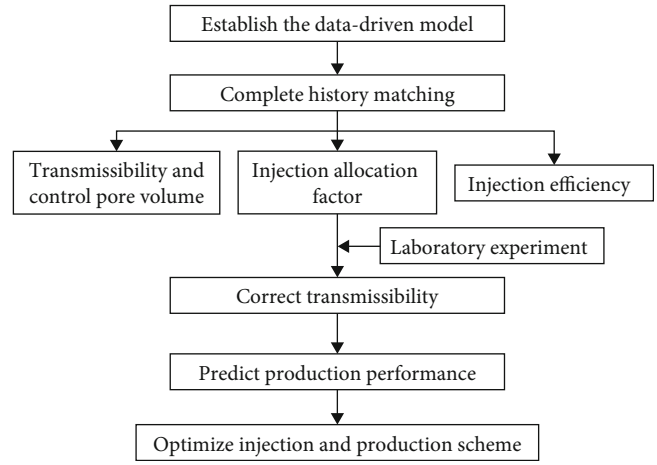

Figure 5: The workflow of the proposed method.

time step is Δt; the difference equation is expressed as follows:

$$p_i^{n+1} - p_i^n = \frac{\Delta t^{n+1}}{\sum_{k=1}^{N_l} C_{t,k} V_{p,i,k}^{n+1}} \left(\sum_{k=1}^{N_l} \sum_{j=1}^{N_w} T_{i,j,k} p_j^{n+1} - p_i^{n+1} \sum_{k=1}^{N_l} \sum_{j=1}^{N_w} T_{i,j,k} + q_i^{n+1} \right). \tag{4}$$

By constructing and solving the pressure equation set (Equation (5)), the pressure in drainage area average of each well point p_i^{n+1} is calculated. The number of equations is identical to the number of wells, rather than the number of grids in traditional numerical simulation, therefore resulting in significant improvement in calculation speed.

$$\begin{pmatrix} G_1^n + 1 & -E_1^n T_{1,2}^{n+1} & \cdots & -E_1^n T_{1,N_w}^{n+1} \\ -E_2^n T_{2,1}^{n+1} & G_2^n + 1 & \cdots & -E_2^n T_{2,N_w}^{n+1} \\ \vdots & \vdots & \ddots & \vdots \\ -E_{N_w}^n T_{N_w,1}^{n+1} & -E_{N_w}^n T_{N_w,2}^{n+1} & \cdots & G_{N_w}^n + 1 \end{pmatrix} \begin{pmatrix} p_1^{n+1} \\ p_2^{n+1} \\ \vdots \\ p_{N_w}^{n+1} \end{pmatrix} = \begin{pmatrix} p_1^n \\ p_2^n \\ \vdots \\ p_{N_w}^n \end{pmatrix} + \begin{pmatrix} M_1^n \\ M_2^n \\ \vdots \\ M_{N_w}^n \end{pmatrix}. \tag{5}$$

Assume that well i and well j are interconnected by connected units, and the pressure of well j is higher than that of well i. Therefore, the flux $(q_{i,j,k}^{n+1})$ of the connected unit between well i and well j in the k-th layer is

$$q_{i,j,k}^{n+1} = T_{i,j,k} \left(p_j^{n+1} - p_i^{n+1} \right). \tag{6}$$

Equation (6) gives the flux distribution in the connected unit, and the saturation is calculated [14]

$$f_w' \left(S_{w,i,j,k}^{n+1} \right) = \min \left\{ f_w' \left(S_{w,j,k}^{n+1} \right) + \frac{1}{C_{v,i,j,k}}, f_w' \left(S_{w,i,k}^n \right) \right\}. \tag{7}$$

Equation (7) gives the derivatives of water cut in different connected units, and the exact water cut can be calculated by interpolation. The comprehensive water cut $f_{w,i,k}^{n+1}$ of well i at the k-th layer is

$$f_{w,i,k}^{n+1} = \frac{\sum_{j=1}^{N_{wu}} q_{i,j,k}^{n+1} f_{w,i,j,k}^{n+1}}{\sum_{j=1}^{N_{wu}} q_{i,j,k}^{n+1}}. \tag{8}$$

Once the water cut of each single well is calculated, other production indexes such as daily oil/water production and

cumulative oil/water production are thereafter can be acquired. Therefore, the rapid prediction of reservoir production dynamics is realized.

The initial values of connectivity parameters are closely related to well physical properties, average permeability, effective thickness, etc. Details are given in the literature [14]. Meanwhile, to match the simulation results with the real production dynamics, SPSA algorithm is applied to assist the history matching method to derive the interwell transmissibility and control pore volume [23]; the iterative formula is

$$m^{l+1} = m^l - \gamma \nabla F\left(m^l\right), \quad m = \left[\cdots, T^0_{i,j,k}, V^0_{p,i,j,k}, \cdots\right]. \tag{9}$$

3. Optimization of Profile Control Parameters

After the interwell connectivity and connected volume are obtained by the multilayer INSIM data-driven model, the parameter optimization method for profile control operation considering the functional mechanism of plugging agent is established. The details are as follows. (1) Select the low-efficiency/inefficient injection well as the objective by analyzing the water injection efficiency and divide coefficient. The values are generated from the physical data-driven model corrected by history match. (2) Calculate the injection volume of plugging agent in each connected unit based on the divide coefficient between the profile control well and the surrounding connected units. The initial volume of the plugging agent being injected is an adjustable input. (3) Update the connectivity parameters after profile control operation. For particle-type plugging agents, laboratory profile control experiments are implemented to find the correlation between plugging agent injection volume, permeability/porosity change, and plugging agent swept volume and to determine the imaginary well locations; therefore, the new connectivity parameters are calculated. For continuous profile control agents like polymer and SMG, the connectivity parameters, permeability, and porosity after profile control operation are updated following the methods offered in published works. (4) Optimize the profile control parameters. Input the updated connectivity parameters into the INSIM data-driven model, set NPV as the objective function, and use the SPSA algorithm to optimize the plugging agent injection volume and injection-production parameters.

3.1. Calculation of Allocation Factors and Selection of Profile Control Well. Assume that well j is the injection well in the k-th layer, and well i is the production well interconnected to well i. Injection divide coefficient defined by Equation (10) is the ratio between the total injection volume and the volume being injected into the interconnected units.

$$A^{n+1}_{j,i,k} = \frac{q^{n+1}_{i,j,k}}{\sum_{i=1}^{N_{wc}} q^{n+1}_{i,j,k}}. \tag{10}$$

Water injection efficiency is defined as the oil being displaced from the surrounding production wells by one PV (pore volume) water, which can be expressed as

$$W^{n+1}_{e,j,k} = \frac{\sum_{i=1}^{N_{wc}} q^{n+1}_{i,j,k}\left(1 - f^{n+1}_{w,i,j,k}\right)}{\sum_{i=1}^{N_{wc}} q^{n+1}_{i,j,k}}. \tag{11}$$

Compare the single-well water injection efficiency (W_e) with the average water injection efficiency of the field block ($W_{e,\mathrm{ave}}$), and categorize the injection wells into high-efficiency well ($W_e > W_{e,\mathrm{ave}}$) and low-efficiency well ($W_e < W_{e,\mathrm{ave}}$). Meanwhile, taking the injection capability into consideration, wells with high injection capability and low injection efficiency should have the priority to conduct the profile control operation.

3.2. Prediction of Dynamic Performance and Parameter Optimization of Profile Control. Considering the different functional mechanisms of different plugging agents, the values of interwell transmissibility and control pore volume in Equations (1) and (2) are revised. The modified material balance equation is

$$p^{n+1}_i - p^n_i = \frac{\Delta t^{n+1}}{\sum_{k=1}^{N_l} C_{\mathrm{t},k} V^{n+1}_{p,i,k}}\left(\sum_{k=1}^{N_l}\sum_{j=1}^{N_w} T'_{i,j,k} p^{n+1}_j - p^{n+1}_i \sum_{k=1}^{N_l}\sum_{j=1}^{N_w} T'_{i,j,k} + q^{n+1}_i\right). \tag{12}$$

Assume a constant-flow pressure production mode is adopted; the changes in injection and production volume due to profile control operation are described as

$$q^{n+1}_{i,k} = J_{i,k}\left(p^{n+1}_{i,k} - p^{n+1}_{wf,i,k}\right), \tag{13}$$

where $p^{n+1}_{wf,i,k}$ is the flowing bottomhole pressure of i well in the k-th layer; $J_{i,k}$ is the injection-production index of i well in the k-th layer after the treatment, which is obtained by updated connectivity [21]. Combine Equations (13) and (12), Equation (5) is expressed as

$$\begin{pmatrix} G^n_1 + E^n_1 J^n_1 + 1 & -E^n_1 T'^{\,n+1}_{1,2} & \cdots & -E^n_1 T'^{\,n+1}_{1,N_w} \\ -E^n_2 T'^{\,n+1}_{2,1} & G^n_2 + E^n_2 J^n_2 + 1 & \cdots & -E^n_2 T'^{\,n+1}_{2,N_w} \\ \vdots & \vdots & \ddots & \vdots \\ -E^n_{N_w} T'^{\,n+1}_{N_w,1} & -E^n_{N_w} T'^{\,n+1}_{N_w,2} & \cdots & G^n_{N_w} + E^n_{N_w} J^n_{N_w} + 1 \end{pmatrix} \begin{pmatrix} p^{n+1}_1 \\ p^{n+1}_2 \\ \vdots \\ p^{n+1}_{N_w} \end{pmatrix} = \begin{pmatrix} p^n_1 \\ p^n_2 \\ \vdots \\ p^n_{N_w} \end{pmatrix} + \begin{pmatrix} M^n_1 \\ M^n_2 \\ \vdots \\ M^n_{N_w} \end{pmatrix}. \tag{14}$$

Solve Equation (14), follow the above-mentioned procedures, and then take the future well working system as the

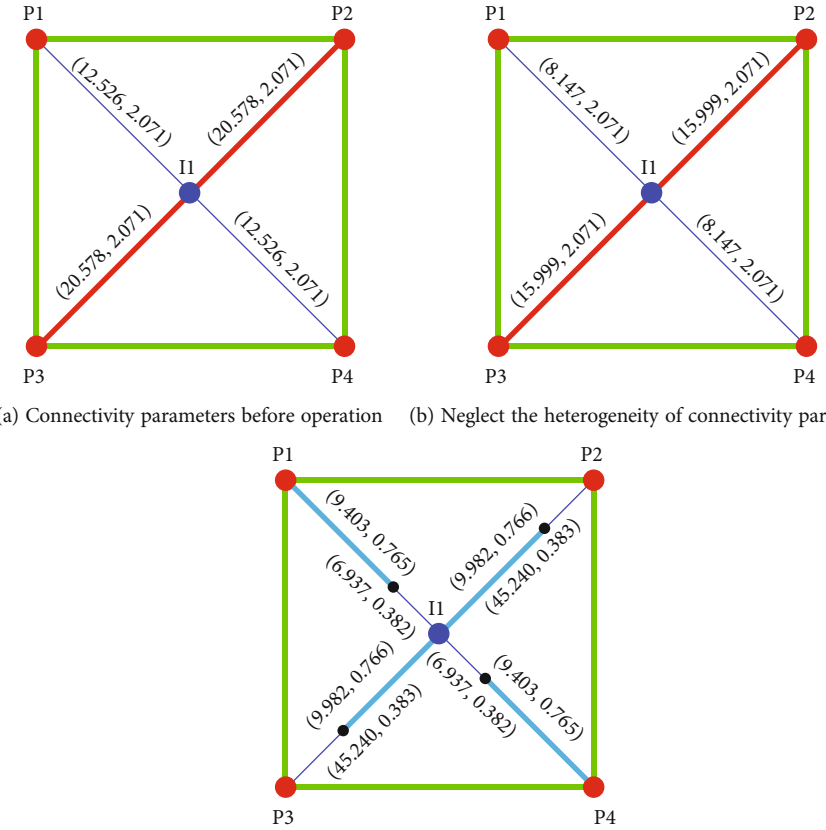

(a) Connectivity parameters before operation (b) Neglect the heterogeneity of connectivity parameters

(c) Consider the heterogeneity of connectivity parameters

Figure 6: Distribution of connectivity parameters in different cases.

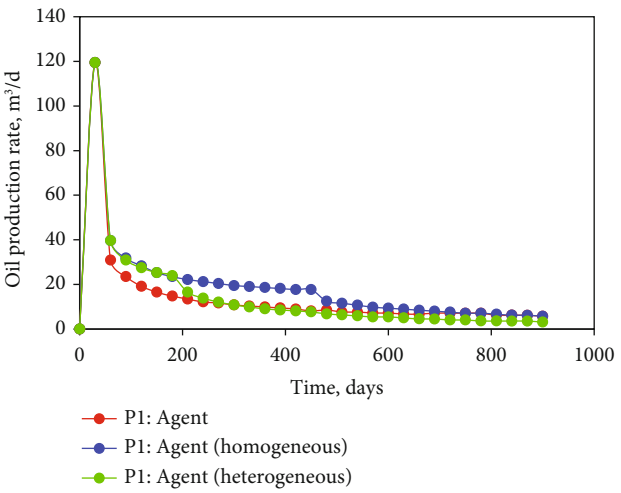

Figure 7: Oil production rates generated by different models.

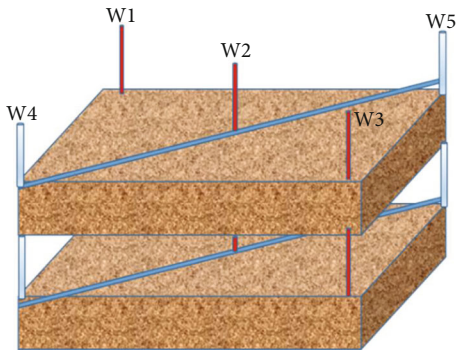

Figure 8: Schematic diagram of the heterogeneous physical model.

control parameter to build the production optimization control model (Equation (15)) with constraint conditions.

$$O(u) = \sum_{n=1}^{L}\left[\sum_{j=1}^{N_P}\left(r_o q_{o,j}^n - r_w q_{w,j}^n\right) - \sum_{i=1}^{N_I} r_{wi} q_{wi,i}^n\right]\frac{\Delta t^n}{(1+b)^{t^n}}. \tag{15}$$

Solve Equation (15) with SPSA algorithm to get the optimal plugging agent injection volume and injection-production parameters. Herein, we give a flowchart to show the steps of this work more clearly, as shown in Figure 5.

4. Model Validation

4.1. Conceptual Model of Profile Control Operation with Particle-Type Plugging Agent. In this section, the typical one injection-four production well group is taken as the example. Figure 6(a) is the distribution of interwell

Table 1: Experimental parameters.

Model	L (cm)	W (cm)	H (cm)	Bulk volume (cm^3)	Φ (%)	Pore volume	k (mD) (channel/matrix)	Initial oil saturation %	Irreducible water saturation %
1	30	30	3.92	3528	34.8	1227.7	1500/500	72.8	27.2
2	30	30	3.86	3474	30.3	1052.6	3000/1000	69.4	30.6

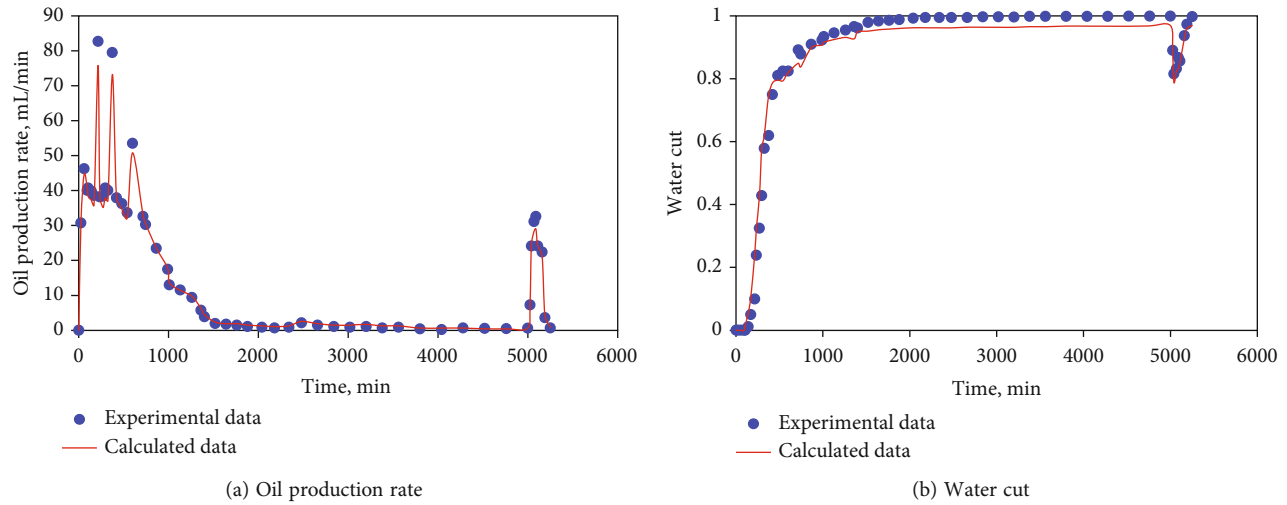

(a) Oil production rate (b) Water cut

Figure 9: Oil production rate and water cut change after polymer profile control.

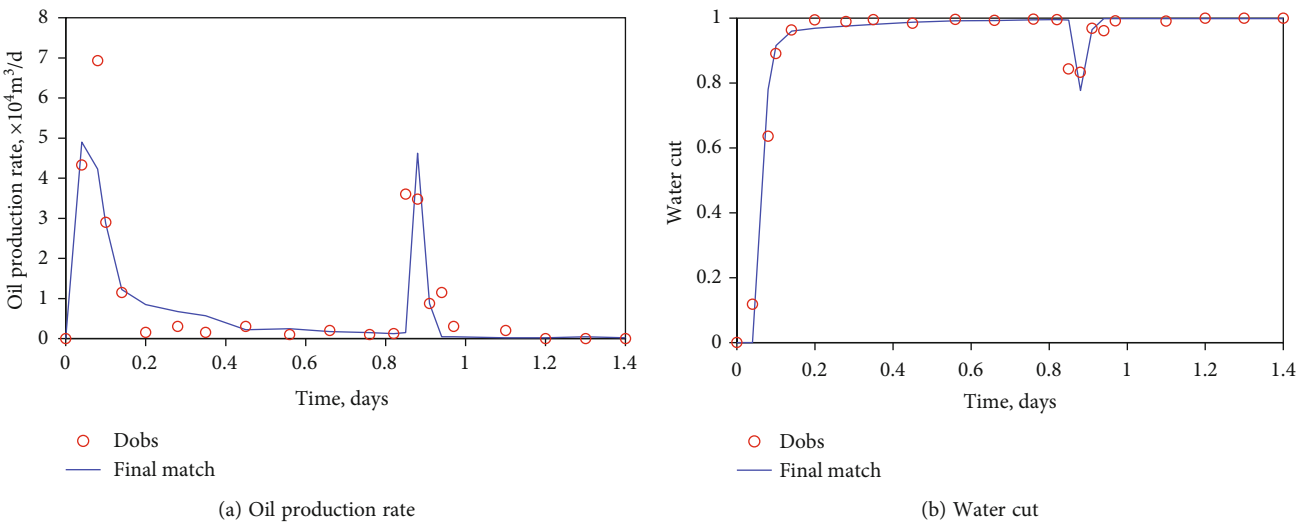

(a) Oil production rate (b) Water cut

Figure 10: Oil production rate and water cut change after SMG profile control.

transmissibility and control pore volume plugging agent injection. Figures 6(b) and 6(c) are the distributions of connectivity parameters after the profile control generated by traditional INSIM model and the novel improved INSIM data-driven model. In traditional INSIM model, the impacts of plugging agent on reservoir percolation ability are learnt from injection divide coefficient of each well and laboratory profile control experiments, while in the updated model, the plugging agent swept volume is also considered and imaginary wells are introduced to model the heterogeneously distributed interwell connectivity parameters. The production rate of each production well is calculated by applying the three sets of connectivity parameters, respectively. The production rate of well P1 is compared in Figure 7. The oil production rate of well P1 increases dramatically after profile control operation because the connectivity and water injection divide coefficient of high permeability channels (P2 and P3) experience huge decreases due to the plugging

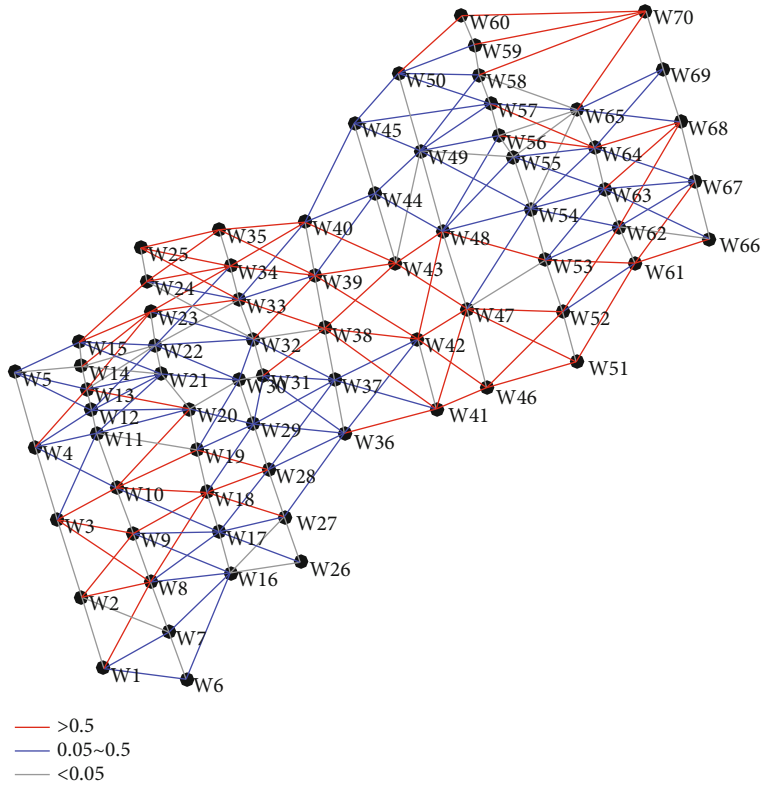

Figure 11: Distribution of interwell transmissibility.

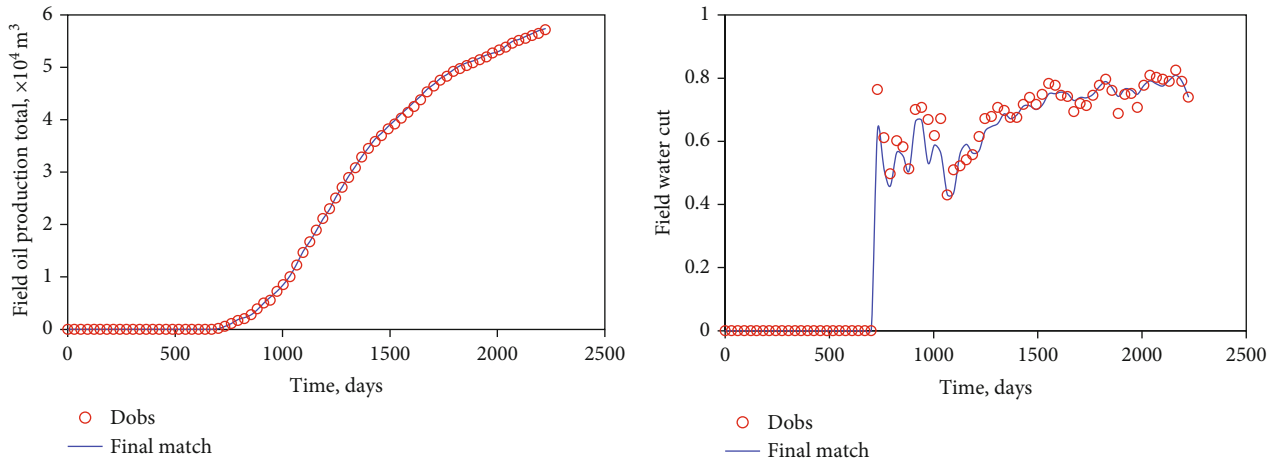

(a) Field oil production total

(b) Field water cut

Figure 12: History matching results of block production indexes.

effects of the injected agent. Therefore, more injected water would divert into the low-permeability channels (P1 and P4) and displace more oil. Meanwhile, it is worth noting that the heterogeneity of the interwell connectivity parameters has noticeable impacts on production dynamics. The production rate in the later production stage would decrease to a similar level to that of before treatment due to the valid period of plugging agent, which is consistent with the real case and also indicates the validity of the model.

4.2. Experimental Verification of Polymer Profile Control. The heterogeneous physical model with high permeability channel is a 30 cm × 30 cm flat core sample with two injection wells (W4, W5) and three production wells (W1, W2,

and W3). As shown in Figure 8, W2, W4, and W5 are located on the high-permeability channel. The displacing rate is set to be a constant of 2 mL/min; other parameters are tabulated in Table 1.

First, inject water into the model from the injection wells, and after 5000 min, inject the polymer solution. The polymer concentration in the produced fluid is measured by titration method with starch and chromium iodide. Increase the test frequency when water cut starts to decrease until the produced polymer concentration reaches the peak. Both the polymer production dynamics and water cut change are monitored.

INSIM data-driven model is also applied to simulate the polymer flooding. Oil production increases obviously and water cut decreases after polymer injection, indicating the positive effects of polymer flooding on profile control and increasing sweep efficiency. The simulation results are consistent with the experimental results, as shown in Figure 9, revealing the feasibility of the proposed model for polymer profile control operation.

4.3. Experimental Verification of SMG Profile Control. The feasibility of the proposed model for SMG profile control operation is also verified by laboratory tests. In this part, parallel core ($d = 2.5$ cm, $L = 10$ cm) flooding experiment is conducted with a high-permeability core and a low-permeability core. Water is injected for 50 minutes, followed by a microgel slug of 0.3 PV. The simulation results generated by the above-mentioned simulation are provided in Figure 10. The oil production rate obviously increases and water cut decreases after microgel injection. The simulation results are consistent with the experimental results, demonstrating the feasibility of the proposed model for SMG profile control operation.

5. Actual Field Application

5.1. Particle-Type Plugging Agent for Profile Control. The newly proposed prediction method for profile control dynamics has been applied in one block of an on-shore reservoir. There are 51 production wells and 19 injection wells. The initial reservoir pressure, average permeability, and average porosity are 23.8 MPa, 58.6 mD, and 0.186, respectively. The derived interwell transmissibility of main production layer is given in Figure 11, where the grey line indicates the transmissibility is smaller than 0.05 m^3/(d·MPa), the blue line indicates the transmissibility located between 0.05 and 0.5 m^3/(d·MPa), and the red line indicates the transmissibility is larger than 0.5 m^3/(d·MPa). The history matching result of field production index is shown in Figure 12; both the field cumulative oil production and water cut match well with the actual production data.

Four low-efficiency/inefficient injection wells are selected for profile control operation based on the derived connectivity parameters. The impacts of plugging agent on formation percolation ability as well as the plugging agent swept volume obtained for field tests and laboratory tests are used in Equation (1) to learn the interwell connectivity change in the swept area and the plugging efficiency can be acquired by

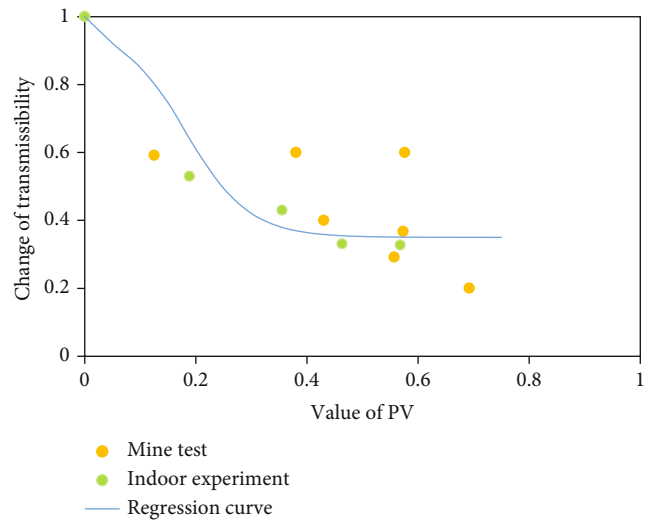

Figure 13: Relation curve of plugging agent injection volume and formation percolation ability.

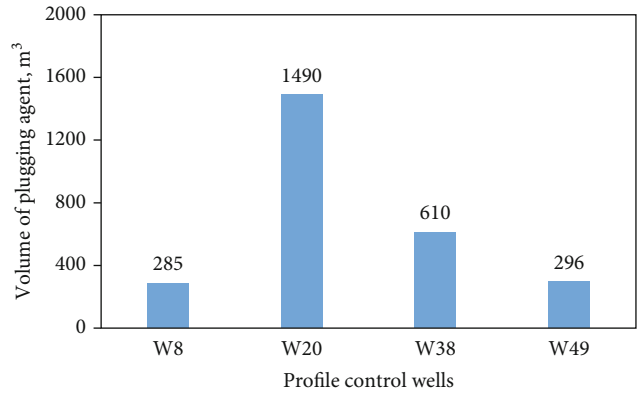

Figure 14: Required plugging agent volume for each profile control well.

multiple regression. As Figure 13 shows, the highest plugging efficiency is 67.28%. The required injection volume for each profile control well given in Figure 14 is calculated by orthogonal test, and the average required injection volume is 670.25 m^3. Figure 15 shows the prediction results of the field oil production rate and field water cut when plugging agent is injected. The data demonstrate an average increase of 1.275 m^3/d in daily oil production rate and a decrease of 3.53% in water cut within. Profile control pilot test on production well W29 gives a 0.634 m^3/d rise in daily oil production rate, which is very similar to the predicted value of 0.58 m^3/d by the novel INSIM data-driven model, showing the high reliability of the proposed method.

5.2. SMG Plugging Agent for Profile Control. After being verified by physical modeling experiment, the prediction method for SMG profile control dynamics has been

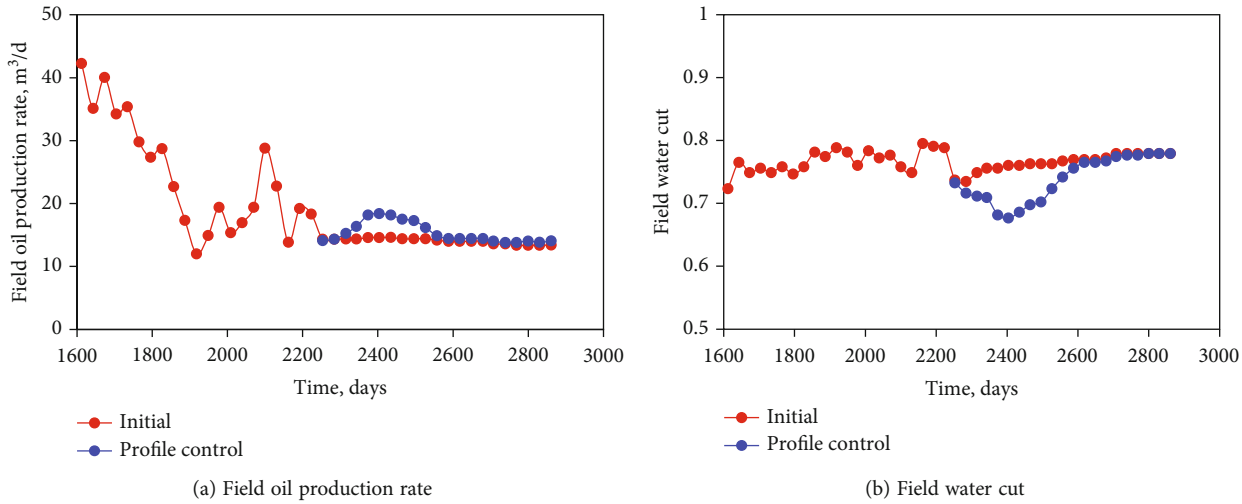

(a) Field oil production rate (b) Field water cut

Figure 15: Dynamic production prediction of profile control of the whole field.

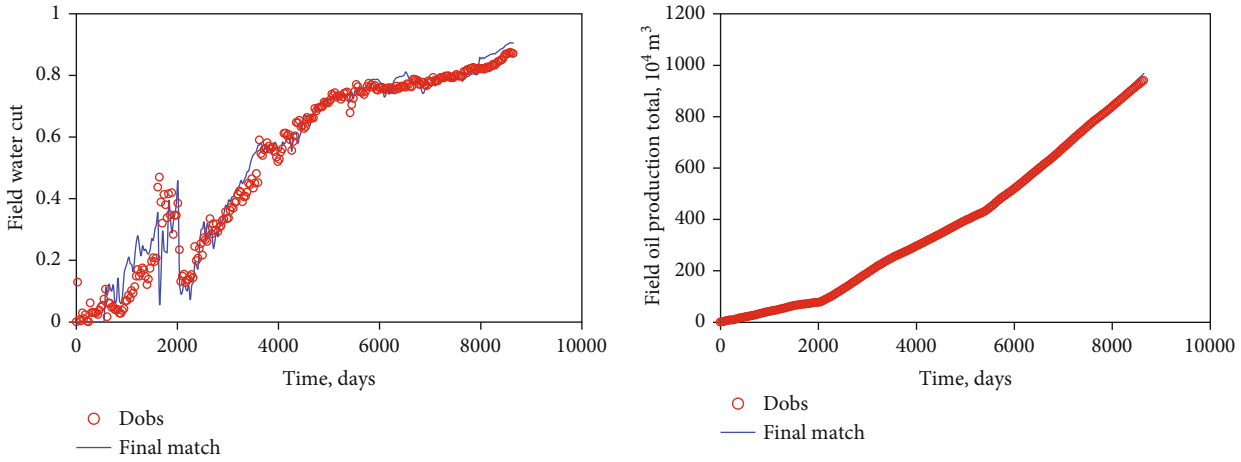

(a) Field water cut (b) Field oil production total

Figure 16: History matching results.

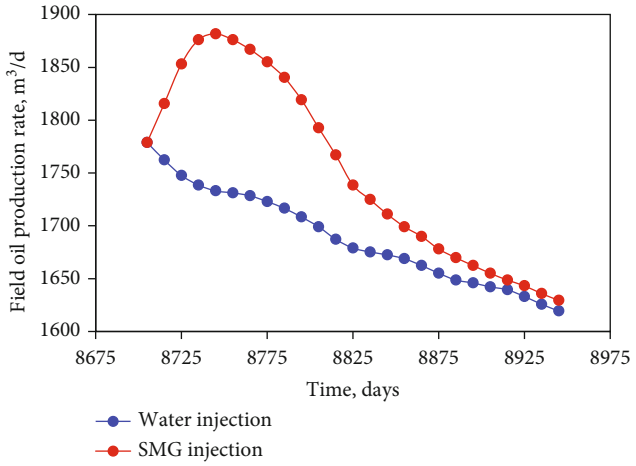

Figure 17: Change in daily oil production after microgel injection.

successfully applied in in one block of an off-shore reservoir. The block went into production in August 1993. There are 65 wells in the target block, including 24 water injection wells and 41 polymer injection wells. The history matching results of single-well production rate, water cut of the block, and the cumulative oil production with actual geological parameters being considered are shown in Figure 16.

The connectivity model corrected by history match is used to predict the profile control dynamics. The changes in daily oil production, cumulative oil production, water cut, and other production indexes within one year are predicted. In this part, two production schemes are simulated and compared in Figures 17–19. In production scheme 1, no changes are made to the current production system at the late production stage, while for production scheme 2, microgel as plugging agent is injected from D6 and D11 (two injection wells) at a concentration of 6000 mg/

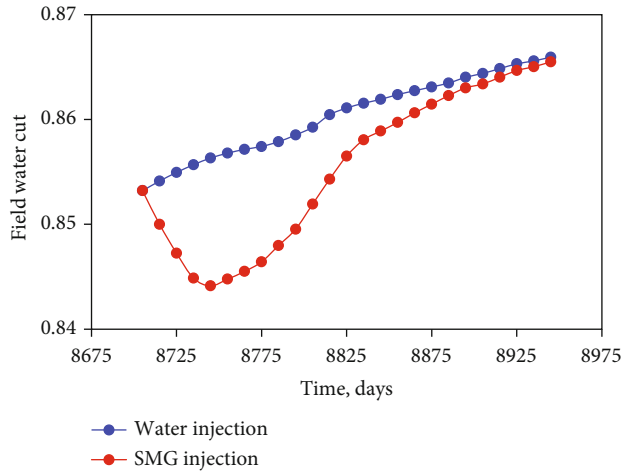

Figure 18: Change in water cut after microgel injection.

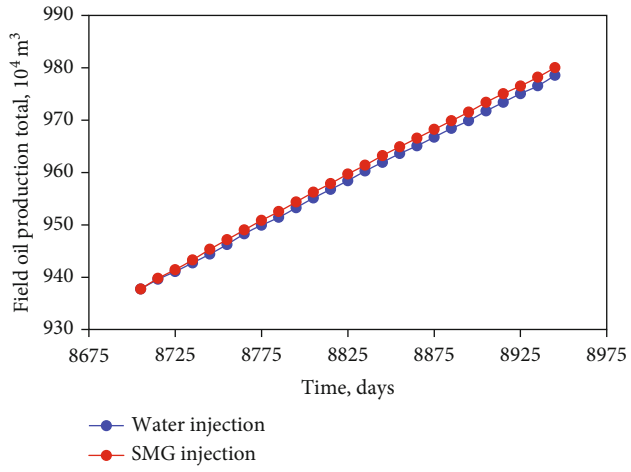

Figure 19: Change in cumulative oil production after microgel injection.

L, where microgel injection would change the interwell connectivity parameters as well as the oil production process.

The oil production rate increases dramatically and then reaches a plateau after 6000 mg/L microgel is injected. The average increase is around 52 m^3/d, and the cumulative oil production increases by 15,000 m^3 within one year. Moreover, the water cut shows a descending trend, which would greatly increase the economic benefit.

6. Summary and Conclusions

(1) Both profile control mechanism and laboratory experimental results are applied in an improved multilayer INSIM data-driven model, and a new prediction method for profile control dynamics in multilayer reservoir considering the heterogeneity of connectivity parameters is established. Meanwhile, a method applying a mathematical model for dynamic optimization of single-well profile control parameters is also proposed

(2) The proposed physical data-driven model eliminates the complicated geological modeling procedure and tedious calculation process associated with the profile control treatment in traditional numerical simulation. The model can also be used to identify the preferential seepage channels without the introducing of high-accuracy seepage flow equations

(3) The reliability of the novel physical data-driven model has been verified by concept examples and experimental data. When being extended to real cases, the optimal plugging agent injection volume for each profile control well is determined and the changes in oil production rate and water cut are predicted. After the profile control operation, oil production increases and water cut decreases. The simulation results are consistent with the real case and can be used to guide the on-site operation

Appendix

A.1. Characterization and Calculation Method of Specific Parameters for Interwell Control Unit

Figure 20 shows a tiny unit in a flow tube, the material balance equation is established with the tiny unit as the object, and the equation is expressed as

$$\frac{k(\xi)}{\mu}A(\xi)\frac{dp}{d\xi} + q(\xi) = \phi(\xi)C_tA(\xi)d\xi\frac{dp}{dt}. \tag{A.1}$$

We perform lateral integration along the flow tube to obtain the flow control equation in a single flow tube as

$$\frac{(1/\mu)(p_i - p_w)}{\int_x d\xi/(k(\xi)A(\xi))} + \int_x q(\xi) = \phi C_t\int_x \phi(\xi)A(\xi)d\xi\frac{dp}{dt}. \tag{A.2}$$

Then, we perform longitudinal integration along the flow tube to obtain the flow control equation in the drainage area of a single well as

$$\int_0^{\alpha_0}\frac{h}{\mu\left(\int_{X1}(d\xi/k(\xi)\xi_1) + (\alpha_m/\beta_m)\int_{X2}d\xi/(k(\xi)\xi_2)\right)}d\alpha(p_i - p_w) + q_i = C_th\frac{dp}{dt}\int_0^{\alpha_0}\left(\int_{X1}\phi(\xi)\xi_1d\xi + \frac{\beta_m}{\alpha_m}\int_{X2}\phi(\xi)\xi_2d\xi\right)d\alpha. \tag{A.3}$$

Comparing Equation (A.3) with the material balance equation [21], the calculation expressions for transmissibility $T_{i,j,k}$ and control pore volume $V_{p,i,k}$ shown in Equations (1) and (2) can be obtained.

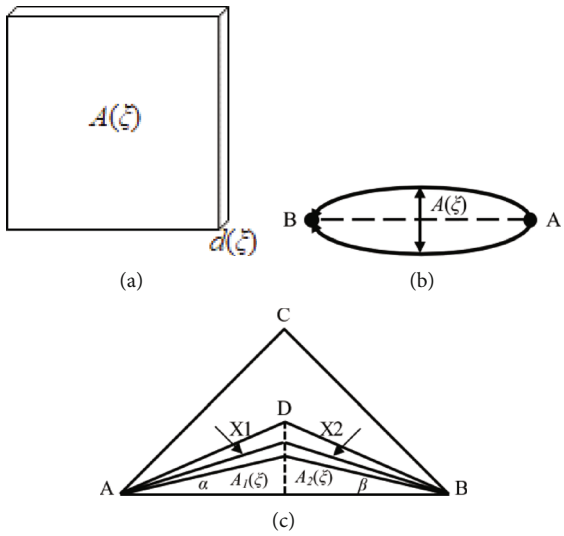

FIGURE 20: (a) Tiny unit. (b) Flow control area of a single flow tube. (c) Drainage area of single well.

Nomenclature

N_l: Layer number
N_w: Injection and production well number
$T_{i,j,k}$: Average transmissibility of well i and well j at the k-th layer (m^3/(d·MPa))
$T'_{i,j,k}$: Average transmissibility of well i and well j at the k-th layer after correction (m^3/(d·MPa))
p_i: The average pressure in the oil drainage area of well i (MPa)
p_j: The average pressure in the oil drainage area of well j (MPa)
q_i: Well flow rate of well i (injection is positive, production is negative) (m^3/d)
t: Production time (d)
$C_{t,k}$: Total compressibility of the k-th layer in reservoir layer (MPa^{-1})
$V_{p,i,k}$: Control pore volume of well i at the k-th layer (m^3)
E_i^n: Intermediate variable, $E_i^n = \Delta t^n / \sum_{k=1}^{N_l} C_{t,k} V_{p,i,k}^n$
$T_{i,j}^n$: Intermediate variable, $T_{i,j}^n = \sum_{k=1}^{N_l} T_{i,j,k}^n$
G_i^n: Intermediate variable, $G_i^n = E_i^n \sum_{j=1}^{N_w} T_{i,j}^n$
M_i^n: Intermediate variable, $M_i^n = E_i^n q_i^n$
$q_{i,j,k}$: Liquid rates between well i and well j at the k-th layer (m^3/d)
f_w: Water fractional flow (f)
$f_{w,i,j,k}$: Water fractional flow of well i at the k-th layer from well j (f)
$f_{w,i,k}$: Composite water fractional flow of well i at the k-th layer (f)
$S_{w,i,k}$: Water saturation of well i in the k-th layer (f)
$S_{w,j,k}$: Water saturation of well j in the k-th layer (f)
$S_{w,i,j,k}$: Water saturation tracking from well j to well i at the k-th layer (f)
$C_{v,i,j,k}$: The cumulative number of pore volumes of fluid from well j to well i, which can be obtained by summing all the instantaneous flow rate of connecting unit $q_{i,j,k}^n$ at every moment
N_{wu}: The number of upstream wells of the i well in the k-th layer
m: Model parameter, vector
n: Time step
γ: Iteration step length
∇F: Simultaneous perturbation gradient
l: Iteration step
$A_{j,i,k}$: Water injection allocation factor from well j to well i in the k-th layer
N_{wu}: The number of upstream wells of the i well at the k-th layer
$W_{e,j,k}$: Water injection efficiency of well j at the k-th layer
α, β: Streamline deflection direction
α_m, β_m: The maximum streamline deflection direction
μ: Viscosity (mPa·s)
ϕ: Porosity (f)
K: Reservoir permeability (10^{-3} μm^2)
h: Reservoir thickness (m)
O: Objective function for production optimization
L: The total number of simulation time steps
N_p: The total numbers of production wells
N_I: The total numbers of injection wells
r_o: The net revenue generated by oil production ($/$m^3$)
r_w: The costs for water production ($/$m^3$)
r_{wi}: The costs for water/agent injection ($/$m^3$)
$q_{o,j}$: The average oil production rates of the production well j (m^3/d)
$q_{o,w}$: The average water production rates of the production well j (m^3/d)
$q_{wi,i}$: The average water/agent injection rate of the injection well i (m^3/d)
b: The annual discount rate (%)
Δt: Time step in day (d)
t^n: The cumulative time up to the n -th year.

Data Availability

The data that support the findings of this study are available from the corresponding author, upon reasonable request.

Conflicts of Interest

The authors declare that they have no conflicts of interest.

Acknowledgments

Hui Zhao would like to express his gratitude to the National Natural Science Foundation of China (Grant No. 51874044 and No. 51922007) for their generous financial support of the research. This study was also supported by the Southern Marine Science and Engineering Guangdong Laboratory (Zhanjiang) (No. ZJW-2019-04).

References

[1] B. Jiang, Q. Ling, and X. Liu, "Application of solid deposition model to water flooding simulation in high pour point oil reservoir," *Acta PetroleiSinica*, vol. 36, no. 1, pp. 101–105, 2015.

[2] Y. Chen and C. Zhou, "Establishment, comparison and application of the linear decline type," *Acta PetroleiSinica*, vol. 36, no. 8, pp. 983–987, 2015.

[3] W. E. Mingqiang, D. U. Yonggang, F. A. Quantang, L. Zhenglan, and L. Anhao, "Production decline analysis method of fractured horizontal well in shale gas reservoirs based on modifying material balance," *Acta PetroleiSinica*, vol. 37, no. 4, pp. 508–515, 2016.

[4] X. Chen, *Study on Migration Laws and Profile Control Numerical Simulation of Gel Particles in Porous Media*, China University of Petroleum (East China), 2015.

[5] Y. Zhou, *Optimization Design of Profile Control and Water Shutoff*, Daqing Petroleum Institut, 2010.

[6] J. Zhang, *The Research and Application of Multiplicity Factor Decision-Making Technique in Block Profile Control and Water Plugging*, China University of Petroleum (East China), East China, 2015.

[7] P. Lian, *Numerical Simulations of Organic Cross-Linking System for Enhancing Oil Recovery*, China University of Petroleum, East China, 2008.

[8] S. Yuan, "A mathematical model of high permeability channel blockage in a heterogeneous reservoir by in-shut polymer gelation process," *Acta PetroleiSinica*, vol. 12, no. 1, pp. 49–59, 1991.

[9] G. Zhang, Q. Feng, D. Tong, Y. Liu, S. Liu, and Y. Chen, "Mathematical model of mobile gel for deep profile control and oil displacement and fast solution methods," *Petroleum Geology and Recovery Efficiency*, vol. 15, no. 4, pp. 55–58, 2008.

[10] F. Qihong, Y. Shiyi, H. Dong, and Y. Shan, "A new method of performance prediction of flowing gel for profile control," *Acta PetroleiSinica*, vol. 27, no. 4, pp. 76–80, 2006.

[11] Z. Rui, J. Lu, Z. Zhang et al., "A quantitative oil and gas reservoir evaluation system for development," *Journal of Natural Gas Science and Engineering*, vol. 42, pp. 31–39, 2017.

[12] Z. Rui, K. Cui, X. Wang et al., "A quantitative framework for evaluating unconventional well development," *Journal of Petroleum Science and Engineering*, vol. 166, pp. 900–905, 2018.

[13] S. Wang, C. Qin, Q. Feng, and F. Javadpour, "A framework for predicting the production performance of unconventional resources using deep learning," *Applied Energy*, vol. 295, article 117016, 2021.

[14] H. Zhao, Z. Kang, X. Zhang, H. Sun, L. Cao, and A. C. Reynolds, "A physics-based data-driven numerical model for reservoir history matching and prediction with a field application," *SPE Journal*, vol. 21, no. 6, pp. 2175–2194, 2016.

[15] Z. Guo, A. C. Reynolds, and H. Zhao, "A physics-based data-driven model for history matching, prediction, and characterization of waterflooding performance," *SPE Journal*, vol. 23, no. 2, pp. 367–395, 2018.

[16] Z. Guo and A. C. Reynolds, "INSIM-FT in three-dimensions with gravity," *Journal of Computational Physics*, vol. 380, pp. 143–169, 2019.

[17] H. Zhao, L. Xu, Z. Guo, Q. Zhang, W. Liu, and X. Kang, "Flow-path tracking strategy in a data-driven interwell numerical simulation model for waterflooding history matching and performance prediction with infill wells," *SPE Journal*, vol. 25, no. 2, pp. 1007–1025, 2020.

[18] X. Xie, H. Zhao, X. Kang, X. Zhang, and P. Xie, "Prediction method of produced polymer concentration based on interwell connectivity," *Petroleum Exploration and Development*, vol. 44, no. 2, pp. 286–293, 2017.

[19] F. Mazlumi, M. Mosharaf-Dehkordi, and M. Dejam, "Simulation of two-phase incompressible fluid flow in highly heterogeneous porous media by considering localization assumption in multiscale finite volume method," *Applied Mathematics and Computation*, vol. 390, article 125649, 2021.

[20] W. Liu, H. Zhao, G. Sheng, H. Andy Li, L. Xu, and Y. Zhou, "A rapid waterflooding optimization method based on INSIM-FPT data-driven model and its application to three-dimensional reservoirs," *Fuel*, vol. 292, p. 120219, 2021.

[21] H. Zhao, Z. Kang, H. Sun, X. Zhang, and Y. Li, "An interwell connectivity inversion model for waterflooded multilayer reservoirs," *Petroleum Exploration and Development*, vol. 43, no. 1, pp. 106–114, 2016.

[22] Y. Zhou, *Evaluation of Hydration Expansion and Plugging Performance of Micro Nano Water Plugging Agent*, China University of Petroleum, Beijing, 2018.

[23] J. C. Spall, "Multivariate stochastic approximation using a simultaneous perturbation gradient approximation," *IEEE transactions on automatic control*, vol. 37, no. 3, pp. 332–341, 1992.

[24] S. Zhou, Q. Zhang, and B. Huang, "Production performance analysis on horizontal wells with variable production index," *Acta PetroleiSinica*, vol. 23, no. 3, pp. 77–80, 2002.

[25] L. Zhang, F. Wang, T. Sun, and B. Xu, "A constrained optimization method based on BP neural network," *Neural Computing and Applications*, vol. 29, no. 2, pp. 413–421, 2018.

[26] X. Li, S. Xiang, P. Zhu, and M. Wu, "Establishing a dynamic self-adaptation learning algorithm of the BP neural network and its applications," *International Journal of Bifurcation and Chaos*, vol. 25, no. 14, article 1540030, 2015.

[27] J. S. Zhao and B. F. Li, "Optimization of profile parameters in steam huff and puff well based on support vector machine," *Journal of Southwest Petroleum University*, vol. 29, no. 5, pp. 53–56, 2007.

[28] C. Cortes and V. Vapnik, "Support-vector networks," *Machine Learning*, vol. 20, no. 3, pp. 273–297, 1995.

[29] L. Saputelli, M. Nikolaou, and M. J. Economides, "Real-time reservoir management: a multiscale adaptive optimization and control approach," *Computational Geosciences*, vol. 10, no. 1, pp. 61–96, 2006.

[30] D. Brouwer and J. Jansen, "Dynamic optimization of waterflooding with smart wells using optimal control theory," *SPE Journal*, vol. 9, no. 4, pp. 391–402, 2004.

[31] G. Nævdal, D. R. Brouwer, and J. D. Jansen, "Waterflooding using closed-loop control," *Computational Geosciences*, vol. 10, no. 1, pp. 37–60, 2006.

[32] H. Asheim, *Optimal Control of Water Drive*, no. article 15978, 1986Society of Petroleum Engineers, 1986.

[33] P. Sarma, L. Durlofsky, and K. Aziz, *Implementation of Adjoint Solution for Optimal Control of Smart Wells*, no. article 92864, 2005Society of Petroleum Engineers, 2005.

[34] C. Wang, G. Li, and A. C. Reynolds, *Production Optimization in the Context of Closed-Loop Reservoir Management*, Society of Petroleum Engineers, 2007.

[35] G. Gao, G. Li, and A. C. Reynolds, "A stochastic optimization algorithm for automatic history matching," *SPE Journal*, vol. 12, no. 2, pp. 196–208, 2007.

[36] Y. Chen, D. S. Oliver, and D. Zhang, "Efficient ensemble-based closed-loop production optimization," *SPE Journal*, vol. 14, no. 4, pp. 634–645, 2009.

[37] Y. Chen and D. S. Oliver, "Ensemble-based closed-loop optimization applied to Brugge field," *SPE Reservoir Evaluation & Engineering*, vol. 13, no. 1, 2010, 2010.

[38] A. L. Custodio and L. N. Vicente, "Using sampling and simplex derivatives in pattern search methods," *SIAM Journal on Optimization*, vol. 18, no. 2, pp. 537–555, 2007.

[39] M. J. D. Powell, "The NEWUOA software for unconstrained optimization without derivatives," in *Large-scale nonlinear optimization*, pp. 255–297, Springer, 2006.

[40] K. Zhang, Y. Chen, L. Zhang et al., "Well pattern optimization using NEWUOA algorithm," *Journal of Petroleum Science and Engineering*, vol. 134, pp. 257–272, 2015.

[41] A. C. David, *An Introduction to Genetic Algorithm for Scientists and Engineers*, Worldscientific, 1999.

[42] R. Eberhart and J. Kennedy, "A new optimizer using particle swarm theory," in *Sixth Symposium on Micro Machine and Human Science*, pp. 39–43, Nagoya, Japan, 1995.

[43] J. M. Pedersen, P. D. Vestergaard, and T. Zimmerman, "Simulated annealing based seismic inversion," *SEG Technical Program Expanded Abstracts*, vol. 1646, 1991.

[44] H. Zhao, C. Chen, S. Do, D. Oliveira, G. Li, and A. C. Reynolds, "Maximization of a dynamic quadratic interpolation model for production optimization," *SPE Journal*, vol. 18, no. 6, pp. 1012–1025, 2013.